Rates of Spontaneous Movement of Water in Capillary Tubes

AYODEJI A. JEJE[1]

Harvard University, Harvard Forest, Petersham, Massachusetts 01366

Received September 20, 1978; accepted December 11, 1978

The neglect of inertia terms and assumption of Poiseuille's flow approximations in describing the motion of a liquid with a free surface in narrow passages are inappropriate for certain motions. This is demonstrated with experiments in which the rates of spontaneous rise of a meniscus in an empty capillary tube, when one end is suddenly contacted with a pool of water, were determined with the aid of a high-speed camera. Glass capillary tubes 266 to 1191 μm in diameter were used in the vertical and horizontal orientations. The results indicate that the mean rise velocity falls steadily with time in a logarithmic fashion for the horizontal arrangement and linearly for the initial stage of vertical rise. Deviations from theoretical predictions in which the assumptions above are made are significant and not similar for the different tube sizes. Actual velocity was initially less than predicted. For vertical rise, the velocity after a while exceeds the prediction at different elapsed times for each tube size. It is suggested that, since the highest Reynolds number (<450) falls within the laminar regime, the flow patterns established are dictated by some stability criteria at the start of the rise.

INTRODUCTION

Although the problem of spontaneous movement of a liquid with free surfaces in capillary tubes has been examined continually over a long period, there is still little quantitative understanding of the event. This status is attributed to two primary reasons: the rapidity of the motion, and the apparently uncontrollable and inconsistent effects of interfacial properties (surface finish at the solid/fluid and contamination at the liquid/gas boundaries) on the advance of the solid/liquid/gas contact line. Huh and Scriven (1) and Templeton (2) presented reviews of much of the relevant literature on the qualitative, and Siegel (3) the limited quantitative, aspects of the problem. An understanding of such flows is of importance in such diverse areas as liquid movements through soils and porous media, textiles and coating processes, and lubrication.

[1] On leave from the Department of Chemical Engineering, University of Lagos, Nigeria.

Flow Descriptions

When the end of an empty capillary is immersed into a pool of a wetting liquid, two menisci are rapidly formed, one on the inside and the other on the outside of the tube. Only the internal meniscus is of present interest. The resulting unbalanced gravity–surface tension force field causes the liquid to rise thereafter at a rate determined by the magnitude of the surface tension force resolved with the prevailing effective contact angle at the contact line. In various studies [(4–6), and others cited by Huh and Scriven], it has been demonstrated that contact angles may vary with both the velocity and direction of meniscus motion; hence it is anticipated that the effective value of surface tension force for the advancing meniscus would increase with decreasing rise velocity for flows against gravity and along the horizontal.

Viscous forces resisting the motion become progressively larger as the wetted wall area increases. For horizontal tubes, gravity

0021-9797/79/060420-10$02.00/0

forces are unimportant, but for vertical orientation and tilt angles in between, the weight of moving liquid column assists or hinders the motion. The latter considerations have led investigators (3, 5, 7–12) to propose variations of the overall momentum balance formulation (following) as describing the flow

$$\frac{2\sigma \cos\theta}{r} - \rho g z - \frac{8\mu}{r^2} z \frac{dz}{dt} - \rho\left(\frac{dz}{dt}\right)^2 - \rho z \frac{d^2z}{dt^2} = 0, \quad [1]$$

where σ, ρ, and μ are the liquid/gas interfacial tension, liquid density, and liquid viscosity coefficient, respectively. The independent variables r, t, and z are the tube radius, time elapsed, and axial distance from inlet, respectively.

A few assumptions have been made to arrive at this expression, probably the most severe of which are those of a constant "pressure" gradient which allows the application of Poiseuille's equation for the viscous term, and the failure to consider the effect of flow profile changes from the curved meniscus to the downstream part by the adoption of a lumped formulation. Further assumptions of constant rise velocity (dz/dt) lead to the neglect of the acceleration term, and contact angles unchanged from the static equilibrium value (usually chosen as zero for water on glass) lead to $\cos\theta$ becoming a constant. The inertia term is routinely dropped to achieve solutions to Eq. [1] in many theoretical efforts.

For very small diameter conduits or with very viscous working liquids, the viscous term may assume the same order of magnitude as surface tension and gravity terms after a short elapsed time. Inertia terms are small. Relatively developed laminar flow, although having transient profiles, is achieved over most of the wetted conduit length with deviations confined to short segments at the entrance region and the immediate wake of the meniscus. Equation [1] then appears to be exact, as the results of Ligenza and Bernstein (11) would suggest.

For larger capillaries, the viscous term is not as prominent, inertia is not negligible, and the effect of assuming Poiseuille's flow becomes significant. Theoretical estimates of rise velocities are higher than those suggested by available experimental data as noted by Rense *et al.* (13, 14) and Siegel (3). In an attempt to explain the discrepancies, subsequent developments have focused on flow dynamics in the neighborhood of the contact line (1, 15, 16).

The Problem

The present effort is an attempt to provide systematic data for the spontaneous movement of water into uniform-bore, vertical, and horizontal capillary tubes of such dimensions that neither Poiseuille's flow assumption is adequate nor can any of the viscous, inertia, gravity, and surface tension terms in the appropriate differential formulation be dropped a priori for the duration of rapid motion. Particular attention is paid to the factors responsible for earlier problems with interfacial effects. The measured meniscus rise rates, $U(t)$, are composed with the values $U^+(t)$ predicted from Eq. [1] for the corresponding capillary orientation when the inertia terms are dropped and a constant (zero) contact angle is assumed [see Levich (10)] through parameter m. Here

$$U^+(t) = \frac{r^2}{8\mu z}\left(\frac{2\sigma}{r} - \rho g z\right) \quad [2]$$

$$m = 1 - \frac{U}{U^+} \equiv 1 - \frac{Re}{Re^+}, \quad [3]$$

with

$$\frac{U}{U^+} = \frac{4\alpha}{1-\beta} \quad \text{for vertical tubes} \quad [4]$$

$$\alpha = \frac{\mu U}{\sigma}\frac{z}{r},$$

$$\beta = \frac{\rho g z r}{2\sigma},$$

and

$$Re = \frac{2rU\rho}{\mu}.$$

For the more general formulation where the inertia term is retained in U^+, an additional dimensionless variable,

$$f = \frac{2\sigma}{\rho U^2 r} \cdot \frac{r}{z}, \qquad [5]$$

is also important. In fact, this represents the friction factor for the horizontal orientation. Factor f relates the maximum capillary pressure attainable to effect the motion ($2\sigma/r$) to the maximum dynamic pressure (ρU^2) that can be developed for a given dimensionless length of penetration (z/r). Parameter m is the deviation of experimental rise rates from predictions based on Eq. [2]. The magnitudes demonstrate clearly the adequacy or inadequacy of applying the equation to capillary flows with free surfaces. Parameter m includes, implicitly, the contributions of the entrance region flows and impulsively started decelerating motion (17), Boussinesq's surface viscosity effects (18) resulting from time-dependent free surface curvature, and the complex flow patterns in the wake of the meniscus (19).

MATERIALS AND METHODS

The apparatus shown schematically in Fig. 1 comprises three basic components: the test capillary, the illumination system, and a high-speed camera. Precision-bore glass capillary micropipets (Becton, Dickinson, and Co., N. J.) 12.5 cm long and of five different internal diameters (ranging from 266 to 1191 μm ± 0.5%) were suspended vertically or laid horizontally above the edge of a glass petri dish 9 cm in diameter and 2 cm deep. The dish was divided into two separate compartments by two Plexiglas plates spaced 4 mm apart, each with two slits 4.5 cm long and 2.5 cm wide, both below the plane of the petri dish edge. The slits in the two plates were oriented on opposite sides so that there was no direct channel between the two compartments. Water introduced at one side traveled a circuitous path through narrow channels to

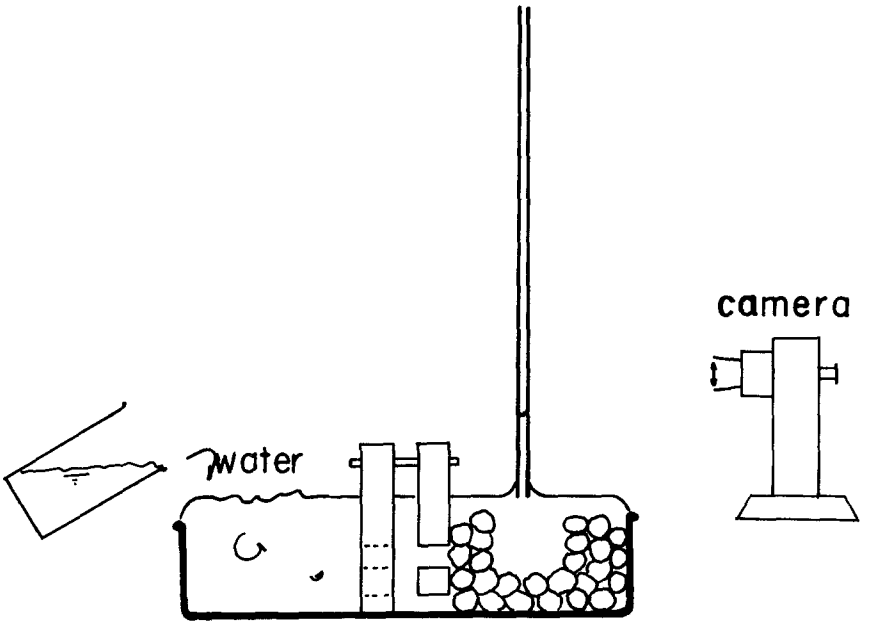

FIG. 1. Schematic of apparatus set-up.

reach the other side; the severe turbulence and free surface oscillations unavoidably generated while rapidly pouring the water were mostly prevented from reaching the test compartment. Any vortices carried over are further dampened by sintered glass beads (~3 mm diameter) arranged in the test section around an open pool (~1.5 cm diameter) directly below the mouth of the capillary. In any experiment all the beads are submerged. The bottom end of the capillary for the vertical orientation is suspended 1 to 2 mm above the plane of the petri dish edge. Apart from being able to include the capillary entrance within the field of view, the arrangement is necessary to minimize the length of capillary that would become submerged and thereby complicate analysis since the pressure head is determined from the plane of the water surface. For the horizontal arrangement, the capillary rests on the dish edge with the entrance protruding more than 1 cm from the edge. The fact that the rounded edge of the petri dish can support about a 2-mm height of water above its plane is utilized in this arrangement. Gravity head is essentially negligible.

Cleanliness of all components of test arrangement is of paramount importance as trace contaminants severely alter the magnitude of the surface tension of water. All samples were initially cleaned with a dilute detergent solution, including the capillary in which indices were moved back and forth several times. This was followed by rinsing many times with distilled deionized water. Warm chromic acid was then applied to all the glass components and rinsed out with distilled water. The capillaries, again full of detergent solution, were kept soaking for a minimum of 24 hr and subjected to ultrasonic vibrations for 5 to 10 min to dislodge adhering solid particles and gas bubbles. This was followed by additional rinses with chromic acid and distilled water, with 2 to 3 min of ultrasonic cleaning. Capillaries were dried out by touching the unused end very lightly to (extra-low monomer content) clean uncoated filter paper until the water column completely receded.

Clean air with a relative humidity of 60 to 90% was then pulled briefly from the capillary end which was not used as the test entrance and the capillary mounted above the petri dish. No water film or droplets were observed even at magnifications of 50× inside the capillaries although the walls were certainly not dry. It is important that no contamination (and minimal dust) touch any part of the test region after this point. It was anticipated that at least a monolayer of water coated the inside walls of the capillary.

At the start of a run, distilled water was introduced into the petri dish to the level of the edge. The capillary was illuminated with a high-intensity tungsten–halogen lamp equipped with a dichroic reflector, via a collimating system of lenses, a 10-cm-thick dilute copper sulphate solution heat filter, a "cold" dichroic mirror which transmits about 80% of incident heat radiation and reflects 90% of visible light, and an infrared glass filter. The high-speed camera, a Redlake HYCAM model equipped with 100/1000-Hz timing light generator, was then actuated at frame rates preset in different runs between 500 and 2000/sec. Corresponding exposure times were 0.8 and 0.2 msec and reproduction ratios were between 0.1 and 2 times. After fractions of 1 sec, a measured quantity of water was rapidly dumped into the nontest section of the petri dish. The water equilibrated in both compartments, and as soon as water touched the capillary tube mouth, meniscus rise commenced and the event was recorded on film. Because only a small quantity of water was dumped, the pool surface approach velocities to the capillary, especially the vertical ones, were estimated to be small. In any case, reproducibility of results relegate this to second-order effects.

Runs at temperatures lower than room value were carried out without special precautions in view of the short duration of

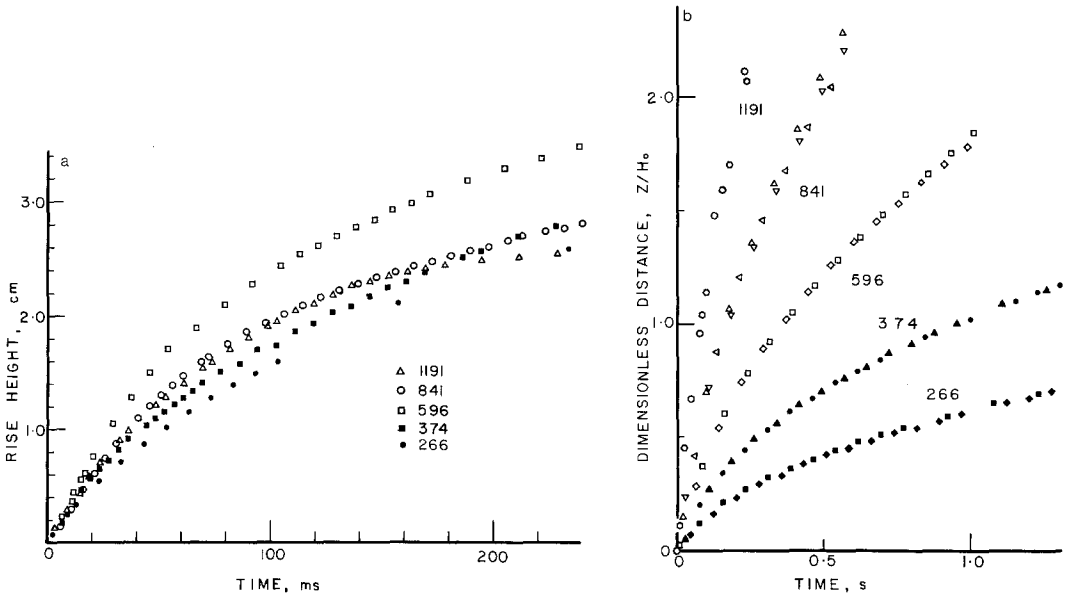

FIG. 2. Typical meniscus distance from inlet versus time elapsed for the different capillary tube diameters, given in micrometers for (a) the vertical orientation, $T_w = 22.8°C$, and (b) the horizontal arrangement, $T_w = 18.5°C$. In (b) the distance has been reduced with $H_0(^2\sigma/\rho gr)$ for scale compression.

the actual measurements. In these cases cold water was used and recorded temperatures were those measured in the pool below the capillary before and after a run. Invariably, because of the high thermal capacity of water, the values were the same. The capillaries were not precooled as moisture condensation from ambient would then present parallax problems.

The films were analyzed frame by frame on a L-W 16-mm data analyzer.

RESULTS

Typical meniscus distance from inlet–time data obtained directly from the films are presented in Figs. 2a and b for runs with water at room temperature in vertical and horizontal capillaries, respectively. In Fig. 2a the initial rise velocities increased from the larger 1191-μm-diameter tubes to the 594-μm ones and then decreased as the capillary diameter became smaller. There are inevitable crossovers between data for the different diameter tubes, for example, the 1191- and 376-μm ones, as might be expected when the large tube is approaching its static equilibrium height while the small one is still far from its ultimate position. Such behaviors are not noted for the horizontal orientation (Fig. 2b).

The raw distance–time data were fitted on the computer with polynomial regression equations up to the 10th order in overlapping blocks for better precision. Both the data and fit equations were plotted to check the behavior of the derived expressions relative to the data before acceptance. The velocities of meniscus rise were then calculated from first derivatives of the regression equations as functions of position. The results are plotted as the Reynolds number versus a dimensionless distance of meniscus from inlet in Figs. 3 to 5. For the vertical orientation the normalization length, $2\sigma/\rho gr$, is that for theoretical static equilibrium (Figs. 3 and 4). The horizontal case theoretically has no steady or limiting state; hence tube radius is used for normalization. A characteristic feature of the plots in Figs. 3 and 4 is that the velocity (or Reynolds' number)

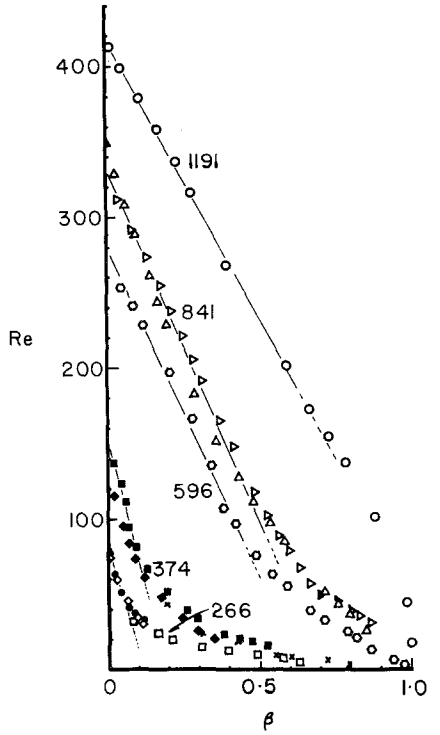

FIG. 3. Reynolds' number versus dimensionless meniscus height β ($\rho^{gzr}/2\sigma$) for spontaneous rise of water in capillary tubes oriented vertically. T_w = 22.8°C. Sizes given in micrometers.

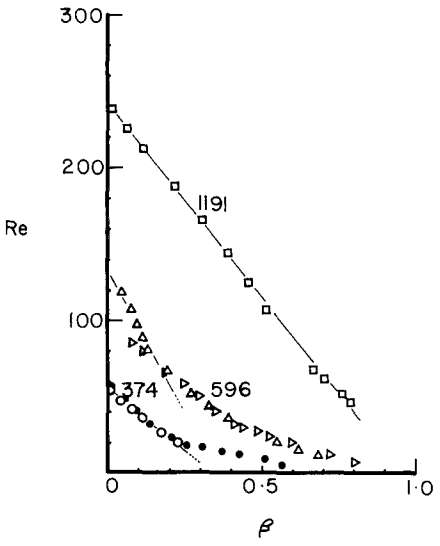

FIG. 4. Reynolds' number versus dimensionless meniscus height β for water at 4°C in vertical capillaries. Sizes given in micrometers.

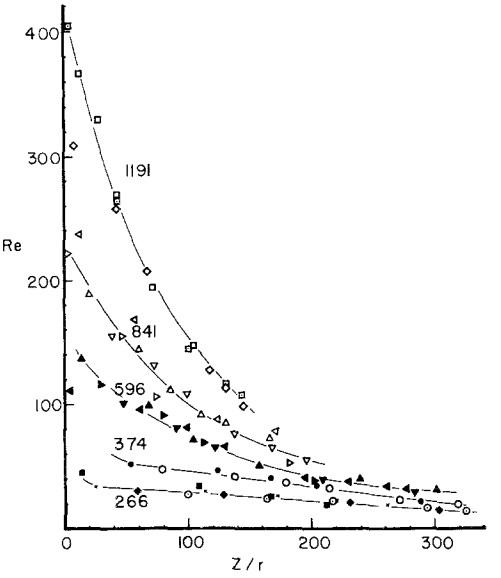

FIG. 5. Reynolds' number versus distance z/r for spontaneous water flow in horizontal capillaries with negligible pressure head. T_w = 18.5°C. Sizes given in micrometers.

drops linearly with distance for the initial portion of the rise. The velocity is not constant. β values at which deviations from this pattern occur decrease with vessel diameter and a lowering of the liquid temperature. The later stages of meniscus rise exhibit a less rapid drop in velocity than earlier observed, except for the 1191-μm-diameter vessel which almost seems to stop abruptly. In some runs the meniscus did overshoot its equilibrium position slightly for the larger tubes. As long as the tube walls were properly cleaned, premoistened, drained of liquid droplets and film patches, and maintained under relatively humid conditions until just before runs, results were reproducible. Occasionally the tubes were not completely drained of water film patches and local velocities of meniscus appear higher than normal. Other times sufficiently high humidity was not maintained, the tube walls partially dried out and the meniscus motion was retarded or stopped completely at spots. Such data are not presented here.

Another feature of the experiments, par-

ticularly with vertical capillaries, is the fact that two menisci are formed. The external meniscus forms almost at the same time as the inner one, although either can rise first. When the internal meniscus rises immediately water touches the capillary, and the external meniscus seems to lag behind up to 50 msec before its contact line slowly (relative to inner meniscus) creeps up the tube to assume its hyperbolic equilibrium profile. Parallax problems for early rise rate measurements of the inner meniscus are presented when the external one rises first. For simultaneous rise, there would be an interaction of flow fields in the neighborhood of the capillary entrance. The effect of such interaction on measured rise rates are judged negligible because of the finite thickness of capillary wall, the sharp corners of ~90° at the capillary mouth, and the very limited height to which the external meniscus ascends.

DISCUSSION

Parameter m has been plotted against dimensionless height β in Figs. 6a and b for water rise at room temperature and 4°C, respectively, in vertical capillary tubes. The plots clearly illustrate the deviation of the experimental results from theoretical estimates disregarding inertia and assuming Poiseuille's profiles. One notes that measured velocity, although initially less, becomes greater than predicted theoretically as seen with the negative m values. In Fig. 3, the data appear to be congregated in three groups spaced apart according to the diameter of the tubes. Although the ratio of the cross-sectional areas in consecutive tube sizes is approximately 2, there are larger

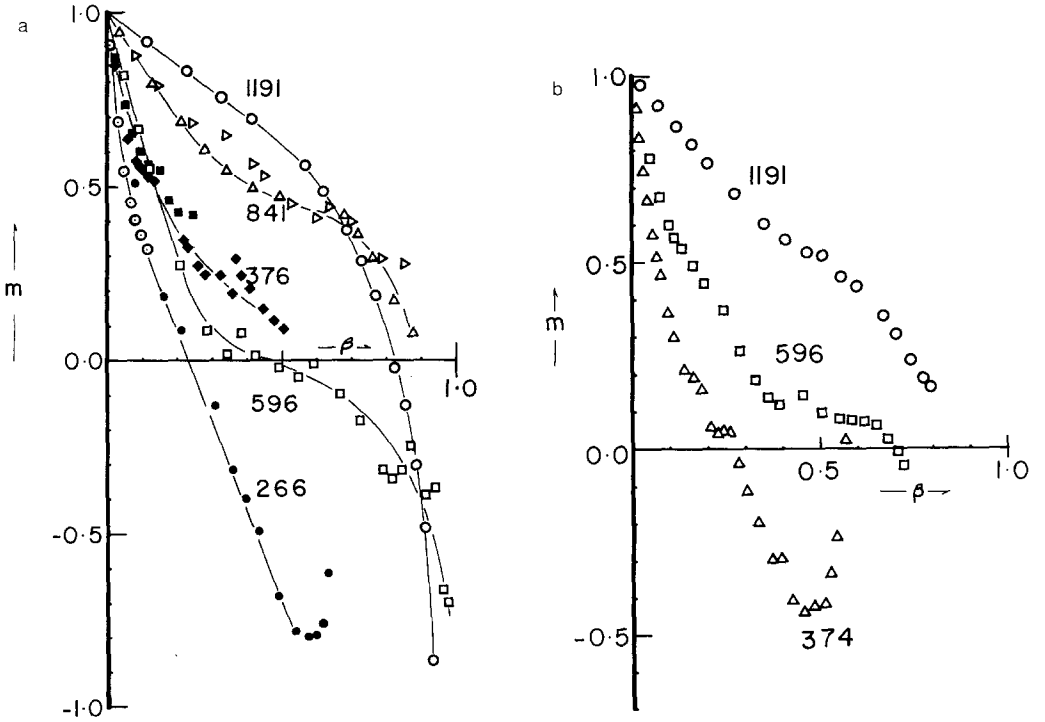

FIG. 6. Plots of velocity deviation parameter m versus dimensionless rise height β for vertical capillary tubes. When the meniscus overshoots its theoretical equilibrium position, m becomes negative infinity. (a) T_w = 22.8°C. (b) T_w = 4°C. With a change in water temperature for a capillary tube, the deviation assumes a pattern similar to the next sized tube at the original temperature. Capillary sizes given in micrometers.

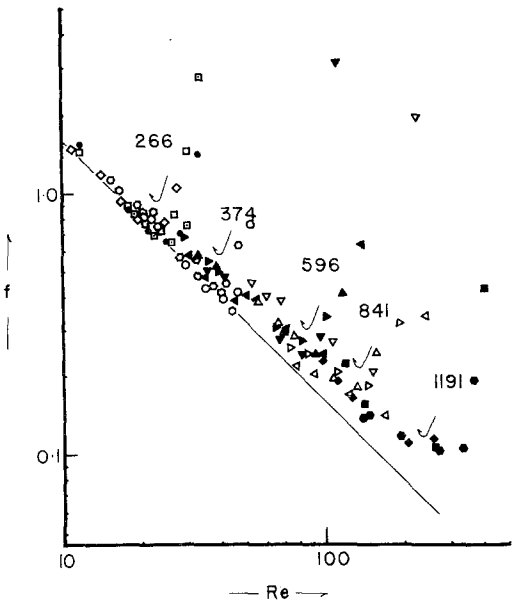

FIG. 7. A plot of friction factor (f) uncorrected for dynamic contact angles versus Reynolds' number (Re) for horizontal capillary tubes at T_w = 18.5°C. The straight line represents theory with inertia terms neglected and Poiseuille's developed laminar flow assumption. Sizes given in micrometers.

separations between data for 1191 and 841-μm-diameter tubes than between the 841- and 594-μm-diameter tubes. Similar observations can be made at the lower end. The shapes of the curves in Fig. 6 also show differences based on a similar pattern for runs at the same temperature. It thus appears that there are three different laminar flow configurations for the capillary sizes investigated since the Reynolds numbers are ~450 and less. Such a possibility has been suggested by LeGrand and Rense (14) and by Stuart (20).

On lowering the water temperature and thereby changing the physical properties, transitions to different laminar flow configurations with vortices appear to occur. This is suggested by a comparison between Figs. 6a and b. Such vortices have been observed (19). The dynamic behavior of capillary rise may then depend on yet-to-be-determined stability criteria established at the start of the motion.

Figure 7 contains a plot of friction factor (uncorrected for the nonzero contact angle) versus the Reynolds number for the horizontal capillaries. Given geometric similarity for meniscus travel in the different capillary tubes, the plots relate the maximum capillary pressure driving the motion to the dimensionless variable which partially describes the flow patterns achieved in the meniscus wake. Reynolds' number defines the conditions for dynamic similarity. Such parameters also permit a comparison of the present data with those for externally driven fully developed laminar flows in capillaries when no free surfaces are present. As compared with steady-state laminar flow predictions (the straight line) the flow resistance for each capillary size started relatively high and then dropped rapidly to a value just above the theoretical line. This initial behavior is attributed both to an overprediction of the driving force by not multiplying the surface tension with the cosine of the instantaneous dynamic contact angle, and the effects of vortex motions (19, 21) behind the meniscus. This may have been partially compensated for by surface tension changes accompanying a free surface creation or its modification (22). After the initial drop, the friction factor increases again but the value lies above the steady laminar prediction. Deviations of data from the $f = 16/Re$ line decreases with vessel diameter and the line represents the asymptotic state for small horizontal capillary tubes.

It is interesting to note that the dimensionless variable $\alpha = (\mu U/\sigma)\cdot(L/r)$ (ratio of viscous and surface tension forces) quickly achieves and maintains for run durations a value between 0.22 and 0.26 at room temperature for horizontal tubes. The values for vertical tubes attained a maximum when the meniscus had traveled between 1.4 and 1.6 cm from the inlet except for the smallest tube when the distance was longer. The maximum α values ranged from about 0.05 for the 1191-μm tube to 0.22 for the 266-μm tube at a distance of about 5.5 cm from the inlet.

The data of LeGrand and Rense (14) have been partly reproduced in Fig. 8 for comparison with the present work. The trends in both results are similar. Of the three capillary sizes they reported (484, 570, and 700 μm diameter) the intermediate size tube showed the highest initial rise rate. Predictable crossover of data for 484- and 570-μm tubes are also noted. However, for similarly sized capillaries higher rise rates are recorded in this work with faster sampling and better precision of photographic methods. The major difference may, however, be the attention paid here to water adsorption on the internal glass walls which apparently minimizes the "stick–slip" phenomenon described by Huh and Scriven (1).

Although the data of Siegel (3) cannot be directly compared with those here because of the difference in experimental conditions, it is informative to examine his Fig. 3 for rise height versus time for seven different vertical tubes, 1.9 to 32.9 mm diameter, immersed in water and then suddenly subjected to zero gravity. This is a variation of the horizontal capillary orientation. Siegel's results show a bunching of data for the smaller tubes (1.9 to 8 mm) in a band while those for 19- and 32.9-mm tubes departed significantly. Is this illustrative of different flow patterns? For the tube sizes used, the initial Reynolds number may have exceeded the critical value for turbulence onset.

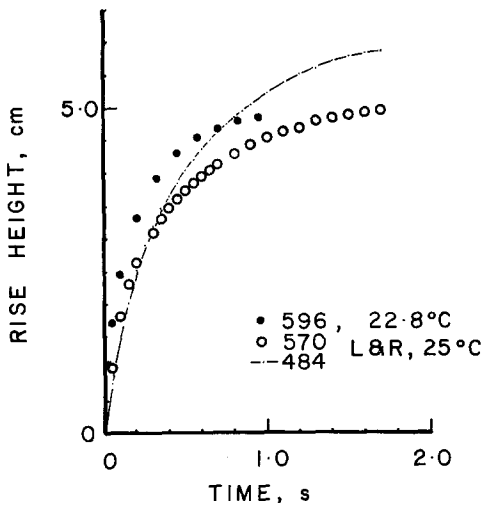

FIG. 8. A comparison of LeGrand and Rense (14) data with a similar run in this study at capillary diameters and water temperatures noted. Capillary sizes given in micrometers.

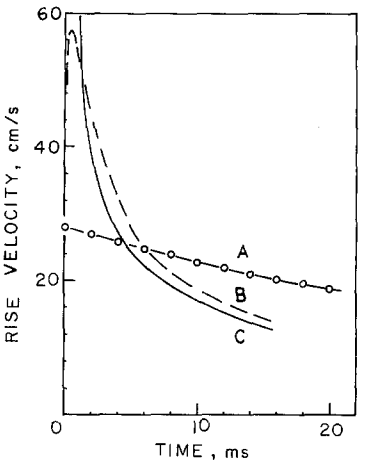

FIG. 9. Comparison of experimental data for water rise rates in 266-μm-diameter capillary (A) T_w = 22.8°C with theoretical predictions from modifications of Eq. [1] (B) and Eq. [2] (C) for 200-μ-diameter capillaries as reported by Szekely *et al.* (23). The theoretical solutions assume a capillary pressure equal to $50/r$.

Finally, the results of the present work are compared with theoretical predictions based on Eq. [1] or its variations. The numerical solutions of Szekely, Neumann, and Chuang (23) capture some essential features of the experimental results, at least for the smallest capillary tubes in the vertical orientation. As shown in Fig. 9 for plots of rise velocity versus time, both the experimental data (for the 266-μm-diameter capillary) and the solution of Szekely *et al.* (for the 200-μm-diameter capillary) exhibit short-time velocities less than those predicted by Eq. [2] (the so called Washburn equation). At $t = 0$, deviation parameter m assumes the value of 1 for both methods. Whereas the maximum velocity appears to have been instantaneously achieved in the experiments, the numerical solution exhibits an acceleration phase with maximum velocity achieved within the 1st msec. The calculated maxi-

mum velocity is a factor of 2 greater than that measured. An arbitrary assumption of ΔP (or $2\sigma \cos \theta/r$) as constant at $50/r$ was made for the calculations. With relation to the experiments, this corresponds to an assumption of a constant dynamic contact angle of approximately 70° or a drastic reduction in surface tension. Available experimental data (19), however, show that in the early rise, the dynamic contact angle undergoes a rapid transition from close to 90° to a value in the neighborhood of the static equilibrium value, 0°. Moreover, capillary waves which rapidly decayed were observed on the meniscus surface soon after inception. These physical differences, not incorporated into the numerical solution, can easily account for the noted differences in maximum velocities.

A short while after the penetration commenced, velocities calculated from both Eqs. [1] and [2] become identical. At different times (~4.5 msec in Fig. 9), the experimental plot also crosses the curve from Eq. [2]. The value for parameter m now vanishes. After these instances, experimental data and the solution of Szekely *et al.* exceed the prediction from Eq. [2]. The maximum deviation of solution to Eq. [1] from that of Eq. [2], $|m|$, in this region is less than 15%.

An increase in the magnitude of ΔP (such as by allowing for a decreasing contact angle) results in an upward shift of both curves B and C relative to A in Fig. 9. (An increase in tube diameter reflects the opposite shift.) Although the errors at short times become exaggerated, the longer time solutions (i.e., greater than 10 msec) approach the experimental values more closely. Discrepancies in velocity attributable to vortex motions in the wake of the meniscus not taken into account in the lumped formulation of Eq. [1] would, however, still persist. For the larger capillary diameters larger errors may be anticipated as Figs. 6a and b would suggest.

ACKNOWLEDGMENTS

Part of this work was carried out while the author held a Bullard Fellowship at Harvard University. Deep appreciation is extended to Professor M. H. Zimmermann, in whose laboratory the experiments were conducted.

REFERENCES

1. Huh, C., and Scriven, L. E., *J. Colloid Interface Sci.* **35**(1), 85–101 (1971).
2. Templeton, C. C., *Petrol. Trans. AIME* **201**, 162–168 (1954).
3. Siegel, R., *J. Appl. Mech.* **83**, 165–170 (1961).
4. Ablett, R., *Phil. Mag.* **46**(6), 244 (1923).
5. Rose, W., and Heins, R. W., *J. Colloid Interface Sci.* **17**, 39–48 (1962).
6. Elliot, G. E. P., and Riddiford, A. C., *J. Colloid Interface Sci.* **23**, 389 (1967).
7. Pickett, G., *J. Appl. Phys.* **13**, 623 (1944).
8. Brittin, E. W., *J. Appl. Phys.* **17**, 37–44 (1946).
9. Barrer, R. M., *Disc. Faraday Soc.* **3**, 61–72 (1948).
10. Levich, V. G., "Physiochemical Hydrodynamics," pp. 382–383, Prentice-Hall, Englewood Cliffs, N. J., 1962.
11. Ligenza, J. R., and Bernstein, R. B., *J. Amer. Chem. Soc.* **73**, 4636–4638 (1951).
12. Washburn, E. W., *Phys. Rev.* **17**(3), 273–283 (1921).
13. Rense, W. A., *J. Appl. Phys.* **15**, 436–437 (1944).
14. LeGrand, E. J., and Rense, W. A., *J. Appl. Phys.* **16**, 843–846 (1945).
15. Ludviksson, V., and Lightfoot, E. N., *AIChE J.* **14**(4), 674–677 (1968).
16. Huh, C., and Mason, S. G., *J. Fluid Mech.* **81**(3), 401–419 (1977).
17. Schlichting, H., "Boundary-Layer Theory," 6th ed. McGraw-Hill, New York, 1968.
18. Scriven, L. E., and Sternling, C. V., *Nature* **187**, 186–188 (1960).
19. Jeje, A., in preparation.
20. Stuart, J. T., *in* "Laminar Boundary Layers" (L. Rosenhead, Ed.), Chap. IX, p. 563. Oxford Univ. Press, London/New York, 1963.
21. Hughes, M. D., and Gerrard, J. H., *J. Fluid Mech.* **50**, 645–655 (1971).
22. Netzel, D. A., Hoch, G., and Marx, T. I., *J. Colloid Interface Sci.* **19**, 774–785 (1964).
23. Szekely, J., Neumann, A. W., and Chuang, Y. K., *J. Colloid Interface Sci.* **35**, 273–278 (1971).